Comparison between Measured and Simulated Antenna Patterns for a LOFAR LBA array

Paola Di Ninni[1], Pietro Bolli[1], Fabio Paonessa[2], Giuseppe Pupillo[3], Giuseppe Virone[2], Stefan J. Wijnholds[4]
[1] Astrophysical Observatory of Arcetri, INAF, Florence, Italy, paola.dininni@inaf.it
[2] Institute of Electronics, Computer and Telecommunication Engineering, CNR, Turin, Italy
[3] Institute of Radio Astronomy, INAF, Bologna, Italy
[4] Netherlands Institute for Radio Astronomy, Dwingeloo, Netherlands

***Abstract*—A UAV-based system has been employed for a measurement campaign on a station of the radio telescope LOFAR to characterize the individual Low Band Antenna patterns. The experimental set-up has been then simulated with a full-wave software and numerical embedded element patterns have been compared to the measured results. A statistical analysis of the differences between the two data sets has been finally carried out to estimate the accuracy of the electromagnetic model.**

***Index Terms*—phased array, mutual coupling, full-wave electromagnetic simulations, UAV-based system.**

I. INTRODUCTION

During last two decades, radio telescopes operating at low radio frequencies have been designed and built on the basis of phased array technology. Following this technology, a radio telescope is composed of a large number of antennas organized as arrays, or stations of the instrument, working as the dishes employed in conventional radio telescopes. The signals received simultaneously from the antennas of a single station are combined to form a unique station beam by means of the beamforming technique.

This technology has been implemented in currently operating radio telescopes, e.g. Low Frequency ARray (LOFAR, www.lofar.org), and it will be used also in the coming low frequency instrument of the Square Kilometre Array (SKA, www.skatelescope.org).

In order to evaluate the functional radio frequency performances of these instruments, including spurious phenomena, like for instance the mutual coupling among antennas and the surrounding environment, electromagnetic software based on full-wave solvers are employed.

A verification of the EM model through an experimental measurement is recommended in order to assess the accuracy and reliability of the numerical results. An experimental system based on an Unmanned Aerial Vehicle (UAV) has been designed and developed by researchers associated to INAF and CNR Italian institutions. This system permits to characterize the angular responses of the single embedded antennas composing the station under test. This technique has been successfully employed in several measurements campaigns [1-3] and recently on a prototype station of the SKA1-Low radio telescope installed at Murchison Radio Astronomy Observatory.

This paper refers to a measurement campaign performed on a station of the Low Band Antennas (LBA), the low frequency subsystem of LOFAR [4] (Fig. 1). In particular, the target of this contribution is to estimate for all individual antennas the differences between simulated and measured patterns and provide some figures of merit of the overall agreement. The comparison between the two sets of data is conducted with a statistical analysis extended to the entire trajectory of the UAV. Furthermore, three frequencies and two configurations of a LBA station have been considered.

Fig. 1. UAV-based system flying during a measurements campaign on a LOFAR LBA station located in The Netherlands.

The paper is organized as follows: the LOFAR LBA station is described in Section II, the UAV-based system is described in Section III and the method to compare experimental and numerical data is reported in Section IV. Finally, Section V and VI illustrate the results of the analysis and the conclusions respectively.

II. LOFAR LBA STATION

A. LBA station

LOFAR is a radio telescope designed by ASTRON and distributed throughout Europe. Stations are geographically distributed mainly in The Netherlands over an area with a

180 km diameter. Each LBA station of LOFAR is composed by 96 antennas and operates as two different sub-arrays known as LBA-inner and LBA-outer array.

The two sub-arrays correspond to different spatial configurations of the antennas: LBA-inner array is composed of 48 dual-polarized antennas distributed within a 30 m circle, while LBA-outer array includes 48 dual-polarized antennas distributed in an annulus with 30 m inner diameter and 85 m outer diameter. The first distribution shows regular features for the central area and random at the array boundary; LBA-outer is, conversely, an array fully randomized (see Fig. 2).

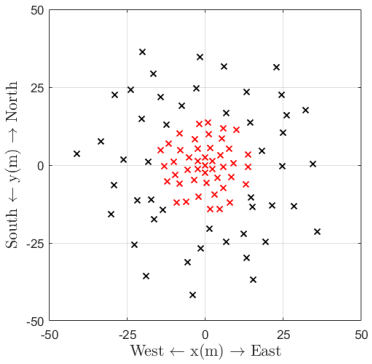

Fig. 2. LBA station configuration: the inner antennas belong to the LBA-inner array (red crosses), while the outermost distribution is the LBA-outer array (black crosses).

B. LBA sensor

The sensor employed in the two LBA sub-arrays consists of two perpendicular inverted V-shaped dipole antennas. Each dipole detects one linear polarization and operates between 30 and 80 MHz. The two perpendicular dipoles are oriented at 45° with respect to the cardinal directions (i.e. a dipole is oriented along the North-East direction, the other one along the South-West direction) and are placed on a metallic wire mesh ground plane of 3 x 3 m^2.

Dipoles are connected to Low-Noise Amplifiers (LNAs) that increase the received signal power level. The signals are thus transported by two separate coaxial cables to the cabinet station, where signals received from all antennas of the station are filtered, amplified, converted to base-band frequencies and finally digitized for data signal processing.

III. UAV-BASED SYSTEM

A. Experimental set-up

The experimental UAV-based system employed to verify the EM models of LBA is composed by a RF transmitter connected to a transmitting dipole installed on the UAV. During a UAV flight, the antennas under test receive a polarized signal emitted as a continuous-wave and, in the meanwhile, an on-board differential Global Positioning System (GPS) measures the position of the transmitting dipole along its trajectory. The UAV angular rotations are measured with an internal inertial measurement unit.

The UAV-based system is extremely flexible since it permits to perform several flights strategies [5] above the array under-test and to select the transmitted frequency and the output power level. For a detailed description of this system see [1].

IV. METHOD

The current section describes both the measurement campaign on a LOFAR LBA station and the corresponding numerical simulations. The figures of merits chosen to define the accuracy of the comparison procedure are briefly illustrated as well.

A. Measurements campaign

The experimental results shown in this paper are based on the measurements carried out applying the UAV-based system to the LBA-inner and LBA-outer arrays of the CS302 core station located in Exloo (The Netherlands) in 2016.

A 2 m long dipole was installed on the UAV resonating in the operating spectral band of LBA. A nominal height of 100 m was selected for the UAV along its complete linear trajectory. For both LBA sub-arrays, the transmitting dipole was aligned to the LBA dipoles along the North-East direction. The UAV height assures that the Far-Field condition applies for the receiving antennas. Complex voltages received by the antennas under test are individually measured as a function of the UAV spatial position along its trajectory.

B. Simulation

The experimental set-up of the measurement campaign has been simulated using FEKO from Altair (www.altairhyperworks.com), a commercial software that performs a full-wave analysis by means of the method of moments. The coupling coefficients, given by the scattering parameters, between the UAV dipole and the antennas under test as a function of the UAV spatial position have been computed [3]. A reference impedance of 50 Ω has been used, while the real values of the LNA impedance have been considered in the data analysis. In particular, the coupling coefficients have been processed [6,7] to include the true impedances of the LNAs: (6.6-j·236.7) Ω, (17.0-j·251.3) Ω and (2.8-j·137.2) Ω at 44, 57 and 70 MHz, respectively.

Decimated UAV spatial positions have been considered and a perfect polarization matching between the transmitting dipole and the antenna under test have been assumed. This assumption is supported since the measured UAV angles are quite close to the nominal angles.

C. Data analysis

Results reported in the next Section for both LBA sub-arrays show the measured and simulated amplitudes of the received complex signals as a function of the UAV spatial position (reported as curvilinear abscissa). The analysis has

been carried out on the RF power received by each array element. Therefore, the pattern of the transmitting dipole and the free-space path-loss have been not removed from the data (the UAV was actually included in the EM model, see section IV.*B*). In order to verify the EM model, the measured and simulated signals have been compared for each antenna of two LBA sub-arrays, separately, at 44, 57 and 70 MHz.

For each antenna, the measured and simulated amplitudes have been normalized and compared point-by-point along the curvilinear abscissa. A weighted logarithmic difference (Δ_w) between the two sets of data have been computed for each antenna as a function of the curvilinear abscissa (see [8] for the weighted difference definition). Furthermore, the average of the weighted difference, avg(Δ_w), and its standard deviation std(Δ_w) are the figures of merit employed in this paper to estimate the discrepancy level between the experimental and numerical data.

V. Analysis of Results

In this Section, the results are presented for LBA-inner array and LBA-outer array. The section is divided in two parts: one discussing the comparison between the simulated and measured antenna patterns and a second one dealing with the statistical analysis of the comparison.

A. Amplitudes comparison

Fig. 4 shows the comparison between the measured and simulated amplitudes for LBA-inner array at 44 MHz for three antennas located in different positions of the array (see Fig. 3). The top panel shows the normalized amplitudes as a function of the curvilinear abscissa for the antennas. Regardless of the measured or simulated data, the three antenna patterns are quite similar each other. However, the mutual coupling effects dependent on the position of each antenna slightly modify the shape of the individual patterns. The shift of the curves along the curvilinear abscissa is due to the spatial position of the UAV with respect to the location of the antennas under test. As far as the agreement between measured and simulated data, the bottom panel shows for the three antennas the weighted differences as a function of the curvilinear abscissa. For the three cases, the weighted differences are between -1 dB and +1 dB.

Fig. 5 is a map that shows the weighted differences for all antenna of the LBA-inner array in every point of the UAV trajectory. It gives a global vision of the levels of the agreement as a function of the antennas and of the curvilinear abscissa. The minimum and maximum values of the Δ_w are between -1 dB and +1.7 dB. At the extremes of the trajectory, the discrepancy between the two sets of data raises to more than 1 dB for almost every antenna, which can be explained by a polarization mismatch, not correctly implemented in the model. Furthermore, far from the origin of the array, the received power is lower and consequently inaccuracies in the model have a larger impact on the results.

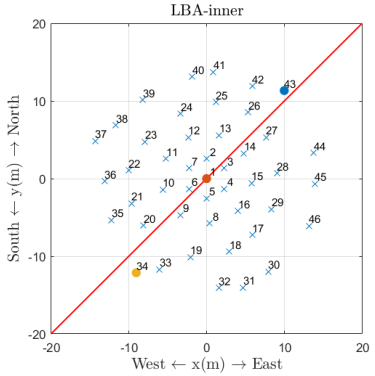

Fig. 3. LBA-inner array: antennas distribution (crosses), antenna index (number from 1 to 46 / antennas 47 and 48 are used for calibration purposes and are located outside this area) and nominal UAV trajectory (red line) are shown. Colored circles indicate the antennas whose amplitudes are shown in Fig. 4.

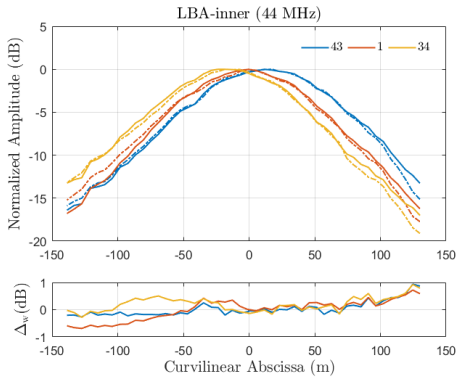

Fig. 4. Comparison between measured (continuous line) and simulated (dashed line) normalized amplitude for three antennas of the LBA-inner array.

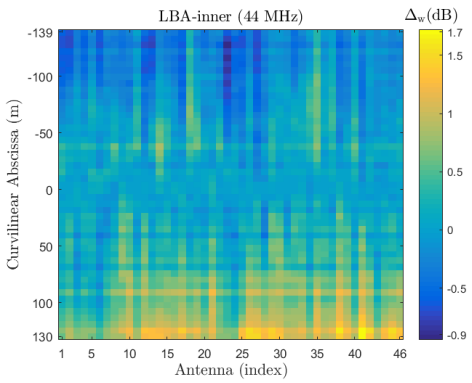

Fig. 5. Weighted differences between measured and simulated normalized amplitudes as a function of the curvilinear abscissa for all antennas of LBA-inner array at 44 MHz.

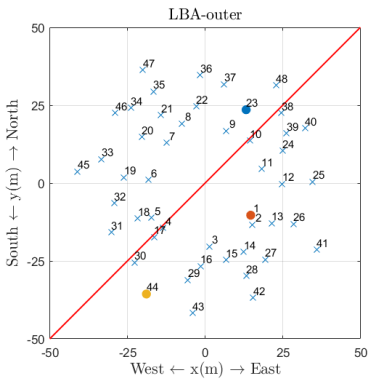

Fig. 6. LBA-outer array: antennas distribution (crosses), antenna index (number from 1 to 48) and nominal UAV trajectory (red line) are shown. Colored circles indicate the antennas whose amplitudes are shown in Fig. 7.

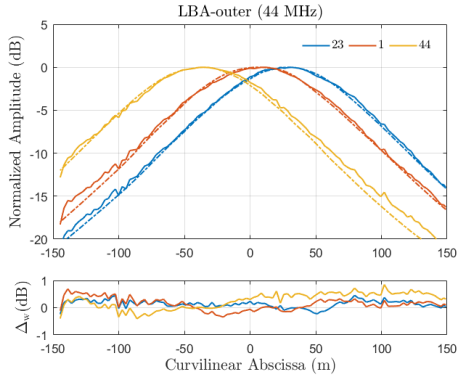

Fig. 7. Comparison between measured (continuous line) and simulated (dashed line) normalized amplitude for three antennas of the LBA-outer array.

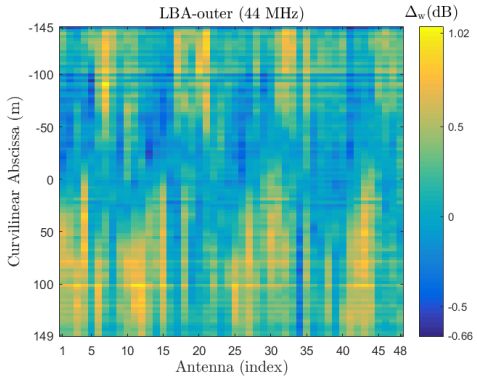

Fig. 8. Weighted differences as a function of the curvilinear abscissa between measured and simulated normalized amplitudes for all antennas of LBA-outer array at 44 MHz

A similar analysis is performed for the LBA-outer. The comparison at 44 MHz between measured and simulated normalized amplitudes is shown in Fig. 7 for the three antennas highlighted in Fig. 6. Here, due to the lower mutual coupling among antennas, the three pairs of patterns turn out to be almost identical. The larger shift of the curves in the LBA-outer with respect to Fig. 4 is due to the higher inter-distance between antennas. Like for LBA-inner array, for the three illustrated cases the weighted differences are between -1 dB and +1 dB. Finally, Fig. 8 displays the weighted differences for all antenna of the LBA-outer array. The minimum and maximum values of Δ_w are in this case between -0.7 dB and +1 dB. The higher accuracy between measurement and simulation for the LBA-outer is likely due to the smoother antenna responses.

B. Statistical analysis

Figs. 9 and 10 show the histograms of the weighted differences for all antennas at 44 MHz of the LBA-inner and LBA-outer array, respectively. This distribution is built by taking into account all values of the weighted differences shown in the previous subsection. The histograms show a symmetric distribution of the errors for both arrays with a standard deviation of 0.43 dB and 0.27 for the LBA-inner and LBA-outer, respectively.

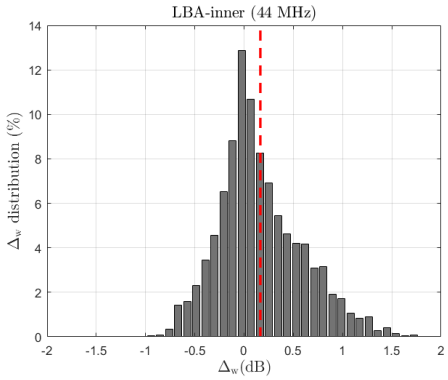

Fig. 9. Distribution of the weighted differences for all antennas of the LBA-inner array at 44 MHz. The red line indicates the average of the distribution.

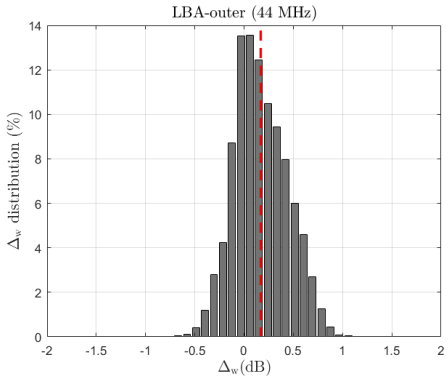

Fig. 10. Distribution of the weighted differences for all antennas of the LBA-outer array at 44 MHz. The red line indicates the average of the distribution.

The analysis at 44 MHz described until now has been repeated at 57 and 70 MHz as well. In Table I, the values of the averages and standard deviations of the weighted differences at the three frequencies have been summarized. The agreement between measurement and simulations is excellent. At 44 and 70 MHz, both LBA sub-arrays have a standard deviation always lower than 0.5 dB, which decreases to 0.3 dB for the LBA-outer. Overall, the LBA-inner array is characterized by a standard deviation larger than the LBA-outer array, which can be explained by the higher mutual coupling effects on the LBA-inner configuration [6] and in turn more sensitive to model inaccuracies.

At 57 MHz, for both LBA sub-arrays the standard deviations slightly increase. At this resonance frequency, the mismatch between the passive antennas and the LNA largely modifies the antenna responses as deeply discussed in [7]. Therefore, small inaccuracies in the estimation of the LNA impedance at this frequency would lead to significant variations in the numerical antenna response.

TABLE I. AVERAGE AND STANDARD DEVIATION OF THE WEIGHTED DIFFERENCES AT 44, 57 AND 70 MHZ FOR THE TWO LBA SUB-ARRAYS

Frequency (MHz)	LBA sub-array	avg(Δ_w) (dB)	std(Δ_w) (dB)
44	LBA-inner	0.17	0.43
	LBA-outer	0.17	0.27
57	LBA-inner	0.05	0.60
	LBA-outer	0.10	0.38
70	LBA-inner	0.20	0.48
	LBA-outer	0.21	0.33

VI. CONCLUSION

A UAV-based system has been used to assess the accuracy of the numerical data for the LBA-inner and LBA-outer arrays. The analysis is performed at array element level by comparing the measured and simulated antenna pattern. The results show that the two sets of data agree very well, with a maximum standard deviation of 0.6 dB, across the operative frequency range and for two different configuration of the instrument.

ACKNOWLEDGMENT

This work has been supported by the 2014 TECNO INAF project “Advanced calibration techniques for next generation low-frequency radio astronomical arrays”.

REFERENCES

[1] G. Virone et al., “Antenna Pattern Verification System Based on a Micro Unmanned Aerial Vehicle (UAV),” IEEE Antennas and Wireless Propagation Letters, vol. 13, pp. 169-172, 2014.

[2] G. Pupillo et al, “Medicina array demonstrator: calibration and radiation pattern characterization using a UAV-mounted radio-frequency source,” Experimental Astronomy, vol. 39, pp. 405-421, 2015.

[3] P. Bolli et al., “Near-Field Experimental Verification of the EM Models for the LOFAR Radio Telescope,” IEEE Antennas and Wireless Propagation Letters, vol. 17, pp. 613-616, 2018.

[4] M. P. van Haarlem et al., “LOFAR: The LOw-Frequency ARray,” Astronomy&Astrophysics, vol. 556, A2, 2013.

[5] F. Paonessa, G. Virone, P. Bolli and A. M. Lingua, “UAV-based antenna measurements: Scan strategies,” 11th European Conference on Antennas and Propagation (EuCAP), Paris, pp. 1303-1305, 2017

[6] P. Di Ninni et al., “Electromagnetic Analysis and Experimental Validation of the LOFAR Radiation Patterns,” International Journal of Antennas and Propagation, vol. 2019, , 2019.

[7] G. Virone et al., “Strong Mutual Coupling Effects on LOFAR: Modeling andIn SituValidation,” IEEE Transactions on Antennas and Propagation, vol. 66, pp. 2581-2588, 2018.

[8] S. Pivnenko et al., “Comparison of Antenna Measurement Facilities With the DTU-ESA 12 GHz Validation Standard Antenna Within the EU Antenna Centre of Excellence,” IEEE Transactions on Antennas and Propagation, vol. 57, pp. 1863-1878, 2009.